Original Article

Microbial Biosystems 10(2) (2025) 2025.355421
0.21608/mb.2025.355421.1238

Contents lists available at Egyptian Knowledge Bank
Microbial Biosystems
Journal homepage: http://mb.journals.ekb.eg/

Characterization of chitosan-based copper nanoparticles: Synthesis approach, antimicrobial activity, and cytotoxicity assay investigation

Ashwaq Abbass Fadhill, Mais Emad Ahmed*

Department of Biology, College of Science, University of Baghdad, Baghdad, Iraq.

ARTICLE INFO

Article history
Received 25 January 2025
Received revised 8 February 2025
Accepted 4 April 2026
Available online 1 June 2025

Corresponding Editors
Hussein Mahdi, Z.
Abdel-Azeem, A. M.

Keywords
Bio-nanotechnology,
cancer cell inhibition,
fungal pathogens,
green synthesis,
polysaccharide-based nanomaterials.

ABSTRACT

This study highlights the synthesis and characterization of copper nanoparticles (Chi-CuNPs) using chitosan, a biopolymer known for its biocompatibility, biodegradability, eco-friendliness, and strong stabilizing properties. The nanoparticles were produced via the solution casting method and characterized using FTIR, UV, SEM, EDX, and XRD techniques, revealing nanomaterials sized between 1–100 nm. Chi-CuNPs exhibited significant antimicrobial activity against multidrug-resistant Gram-positive and Gram-negative bacteria, as well as Candida species. In diffusion assays, inhibition zones ranged from 10–27 mm for bacteria and 22–24 mm for Candida, indicating stronger effects against Gram-positive strains. The nanoparticles also demonstrated notable anticancer activity, especially against the MCF7 human breast cancer cell line and ovarian cancer cells, showing cytotoxic effects at a concentration of 25 µL/mL. These findings suggest Chi-CuNPs have promising potential for antimicrobial and anticancer applications, particularly in tissue engineering and infection control. However, the exact mechanism underlying their antibacterial effects remains unclear, necessitating further investigation. Additional research is essential to establish safe dosage levels and fully explore the therapeutic potential and mechanisms of action of Chi-CuNPs in both clinical and biomedical applications.
.

Published by Arab Society for Fungal Conservation

Introduction

Nanotechnology refers to the science of manipulating matter at the atomic and molecular scale. This cutting-edge field holds the potential to revolutionize numerous industries, particularly medicine (Muzammil et al. 2018).

Among the many applications of nanotechnology, nanoparticles (NPs) offer significant advantages in cancer treatment, including their small size, high surface-to-volume ratio, unique fluorescent properties, enhanced permeability, and remarkable biocompatibility. Compared to other types of nanoparticles, metallic NPs exhibit superior performance and hold significant promise as pharmaceutical agents (Mahdi et al. 2024).

Nanotechnology and nanoparticles also play a crucial role in combating microorganisms and multidrug resistance. Research has demonstrated that nanoparticles containing silver (Ameh et al. 2022), copper (Faiq et al. 2024), and other elements exhibit strong antibacterial effects, including against multidrug-resistant bacteria, whether or not antibiotics are involved (AbdelAzeem et al 2020, Srivastava et al. 2021, Gezaf et al. 2022, Mossa et al. 2024).

There are various methods for synthesizing nanoparticles. Traditional physical and chemical techniques are widely used; however, these approaches often suffer from disadvantages such as high costs,

***Corresponding author Email address**: mais.emad@sc.uobaghdad.edu.iq (Mais Emad Ahmed)

significant energy consumption, the use of toxic chemicals, and the generation of hazardous byproducts (Diksha et al. 2023).

Chitosan (CHT), derived from chitin—the second most abundant natural polymer after cellulose—is found in the exoskeletons of crabs, shrimp, lobsters, corals, squid, jellyfish, insects, fungi, yeasts, and algae. Due to its solubility, chitosan can be produced through several methods (Ahmed et al. 2023). Chitosan is known for its biodegradability, biocompatibility, and antibacterial properties, which inhibit the growth of various microorganisms. These properties depend largely on structural factors such as the degree of deacetylation and molecular weight. Additionally, the extraction source and deacetylation method significantly influence the final physical, chemical, and biological characteristics (Ardila et al. 2017).

One of the primary mechanisms behind chitosan's antimicrobial activity is the presence of positively charged amino groups at pH levels below 6.3, which interact with the negatively charged cell walls of microorganisms. This interaction leads to the leakage of intracellular components, causing cell membrane damage and eventual cell lysis (Tabesh et al. 2019).

Recent studies have focused on creating chitosan-copper nanoparticle coatings on stainless steel to simultaneously improve corrosion resistance and antibacterial properties. The electrophoretic deposition (EPD) technique has been used to develop nanocomposite coatings with varying concentrations of copper nanoparticles, following the synthesis of chitosan-modified copper nanoparticles. The resulting coatings have been evaluated for their antibacterial activity, corrosion resistance, and physicochemical properties in simulated body fluid (SBF) (Tabesh et al. 2019).

Furthermore, chitosan nanoparticles and those loaded with copper (II) have been shown to inhibit the growth of tumor cell lines in a dose-dependent manner. These nanocomposites exhibit remarkable biological activities, including antibacterial, anticancer, and antioxidant properties, indicating their high potential for pharmaceutical applications, particularly in the development of innovative antimicrobial and antioxidant drugs (Ashokkumar et al. 2024).

Given the growing need to design and synthesize new materials with enhanced antibacterial properties, recent research has increasingly focused on the combination of chitosan and copper for this purpose. Numerous studies have demonstrated the effectiveness of chitosan-based metal oxide nanoparticles in diverse applications, particularly for their antimicrobial potential.

The objective of this study is to evaluate the antibacterial efficacy and physicochemical properties of copper nanoparticles based on chitosan. Additionally, the study aims to determine the synergistic effect of combining chitosan and copper within a single nanomaterial and to assess whether their combined antibacterial properties are enhanced.

Material and Methods

Clinical samples and Inocula preparation

Clinical isolates of Gram-negative and Gram-positive bacteria, along with pathogenic fungal strains including *Candida albicans*, *Candida guilliermondii*, and *Candida ferric*, were obtained from the College of Medicine at Iraqi University. Pure colonies from these isolates were suspended in sterile saline, and the turbidity was adjusted to 0.5 McFarland standard, equivalent to approximately 1×10^8 CFU/mL, for all microbiological assays.

Preparation of Chitosan

Chitosan was synthesized through the deacetylation of chitin using 70% sodium hydroxide (NaOH) with a solid-to-solvent ratio of 1:12 (w/v). The reaction was carried out at room temperature with continuous stirring for 74 hours to ensure uniform deacetylation. Following the reaction, the chitosan product was thoroughly washed with running tap water, rinsed with distilled water, filtered, and oven-dried to obtain purified chitosan powder (Fig. 1).

Synthesis of Chitosan-Copper Nanoparticles (Chi-CuNPs)

Chi-CuNPs were synthesized following the procedure described by(Mallick et al. 2012), with slight modifications. One gram of chitosan was dissolved in 100 mL of 1% acetic acid solution. Fifty milliliters of this solution were combined with a copper salt solution and sonicated for 10 minutes before being transferred to a 250 mL round-bottom flask. The addition of 1 mL of 0.6 M NaOH resulted in a color change to bluish, indicating initial nanoparticle formation. After continuous stirring for 20 minutes, 1 mL of hydrazine hydrate was added gradually, leading to a color change from yellow to reddish-brown, confirming the reduction of copper ions. The mixture was stirred for an additional 10–20 minutes, cooled to room temperature, and centrifuged at 5300 rpm. The pellet was washed multiple times with distilled water to remove residual reactants, yielding purified Chi-CuNPs (Fig. 2).

Characterization of Chi-CuNPs

The structural and morphological properties of the synthesized Chi-CuNPs were characterized using several techniques, including scanning electron microscopy

(SEM), transmission electron microscopy (TEM), atomic force microscopy (AFM), dynamic light scattering (DLS), X-ray diffraction (XRD), Fourier-transform infrared spectroscopy (FTIR), UV-visible spectroscopy, and energy-dispersive X-ray spectroscopy (EDX), following the approach of (Romi et al. 2024).

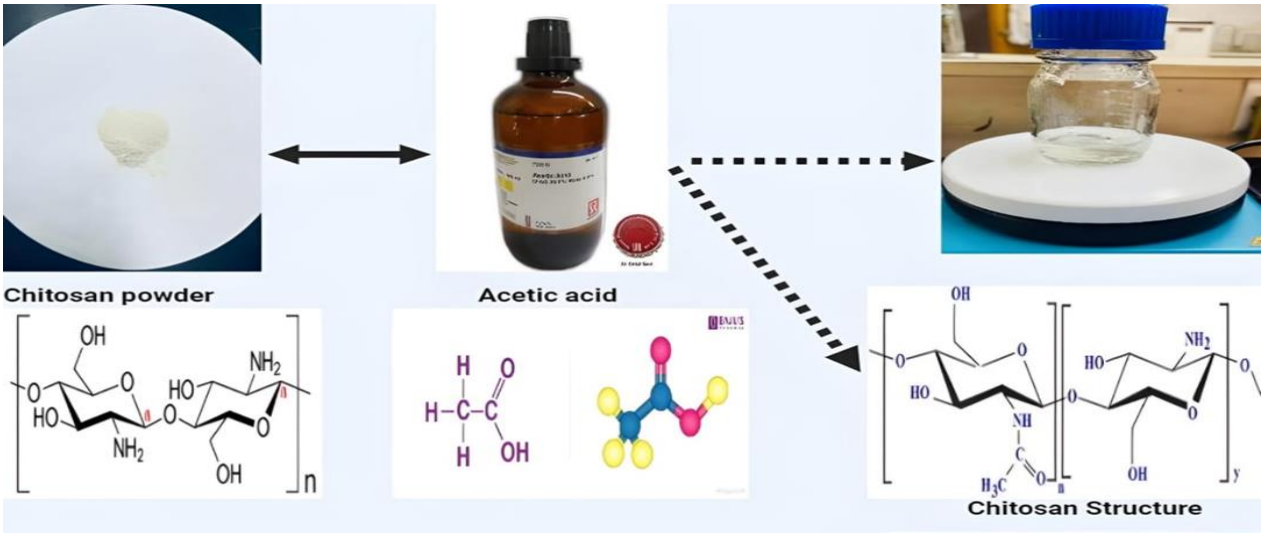

Fig 1. Schematic representation of the preparation process of Chitosan.

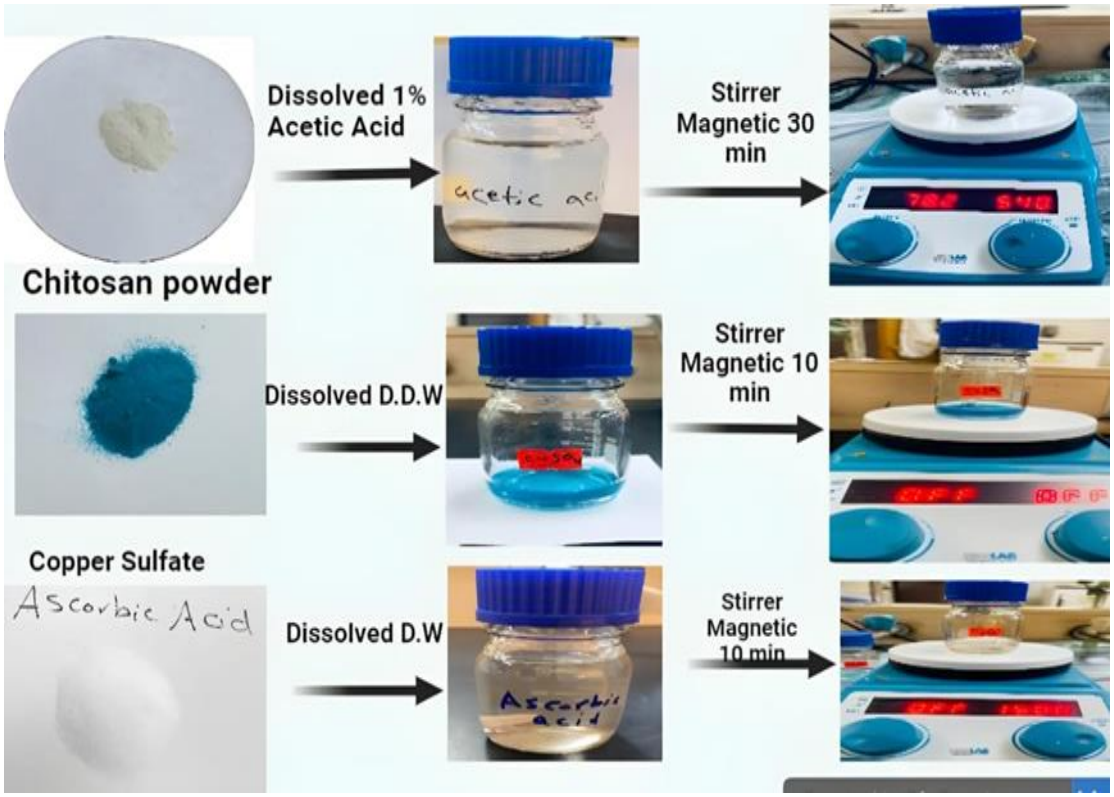

Fig 2. *Schematic illustration of the synthesis process of Chi-CuNPs nanoparticles.*

Evaluation of antimicrobial activity

Agar Well Diffusion Assay

The antibacterial and antifungal activities of Chi-CuNPs were evaluated using the agar well diffusion method, as described by (Kadhim et al. 2023). Mueller-Hinton agar (MHA) plates were inoculated with bacterial suspensions adjusted to 0.5 McFarland standard using sterile cotton swabs. Five wells were created on the agar surface using a sterile borer. Each well was filled with 80 µL of Chi-CuNPs suspension (2000 µg/mL). Control wells included copper acetate, Mueller-Hinton broth (negative control), and ceftriaxone (50 µg/mL) as the positive control. Plates were pre-incubated at 4°C for 30 minutes to allow diffusion, followed by incubation at 37°C for 24 hours. The inhibition zones were measured in triplicate, and results were expressed as mean ± standard deviation (SD) . The Antimicrobial activity was calculated using the following formulas:

$$AI = \frac{(IZD)\ of\ test}{IZD\ of\ standardantimicrobial}$$ ---------(formula 1)

(PI) = AI × 100 ---------(formula 2)

Where "AI" represents the Activity Index, "IZD" represented Inhibition Zone Diameter and "PI" Percentage Inhibition.

Determination of Minimum Inhibitory Concentration (MIC)

The MIC of Chi-CuNPs against bacterial and fungal isolates was determined using the broth microdilution method, following (Fawzi et al. 2024). Indicator strains were cultured overnight, and Chi-CuNPs were serially diluted in the appropriate growth medium to final concentrations of 1000, 500, 250, 125, and 64 µg/mL. Mueller-Hinton broth was used for bacterial cultures, while suitable media were applied for fungal strains. The MIC was defined as the lowest concentration of Chi-CuNPs that inhibited visible microbial growth.

Cell culture and cytotoxicity Assay (MTT Assay)

The human breast cancer cell line MCF7 was used to assess the cytotoxic effects of Chi-CuNPs. Cells were cultured in RPMI-1640 medium supplemented with 10% fetal bovine serum (FBS) and 1% penicillin-streptomycin solution, as per the protocol of Alhammer et al. (2024). Cells were maintained at 37°C in a humidified atmosphere with 5% CO_2. For in vitro assays, Chi-CuNPs were dissolved in deionized water, and working concentrations were prepared in complete RPMI-1640 medium.

The cytotoxic effects of Chi-CuNPs were evaluated using the MTT assay, as described by (Hassan et al. 2024). MCF7 cells (7000 per well) were seeded into 96-well plates and incubated overnight. Cells were then treated with increasing concentrations of Chi-CuNPs ranging from 6.25 to 100 µg/mL, with three replicates per concentration. After 24 hours, the medium was replaced with 20 µL of MTT solution (5 mg/mL), followed by a 3-hour incubation at 37°C in the dark. Subsequently, 50 µL of DMSO was added to each well to dissolve the formazan crystals, and absorbance was measured at 490 nm using a microplate reader. Cell viability was calculated using the (formula 3):

$$\text{Viability}(\%)=\frac{[(\text{A\_test} - \text{A\_blank})}{(\text{A\_control} - \text{A\_blank})]} \times 100$$-----(formula 3)

Where "A" represents the absorbance values for test, blank, and control wells. The dose-response curve and the GI_{50} value (the concentration of Chi-CuNPs required to inhibit 50% of cell viability) were calculated using GraphPad Prism software, version 6, as per the methodology of (Mahdi et al. 2024).

Results

Chemical Synthesis of Chitosan-Copper Nanoparticles (Chi-CuNPs)

The use of biological materials such as chitosan offers an environmentally friendly alternative to conventional physical and chemical methods for the safe, rapid, and cost-effective synthesis of nanoparticles (NPs). In this work, chitosan served as the primary stabilizing and reducing agent during the chemical synthesis of Chi-CuNPs. The appearance of a dark green color during the reduction reaction indicated the successful formation of new nanoparticles (Usman et al. 2012). This characteristic color change results from the ability of chitosan components to interact with metal ions and facilitate their reduction into Chi-CuNPs (Kadhim et al. 2023).

Green copper oxide (CuO) nanoparticles were produced and characterized using chemical methods. The synthesized Chi-CuNPs were subsequently evaluated for their antibacterial properties. Notably, the color changes observed during the formation of copper nanoparticles correspond to specific chemical transformations taking place during the synthesis process. The dropwise addition of bulk copper solution into the chitosan solution initially resulted in a light blue color, indicating the formation of a chitosan-copper complex (Fig. 3).

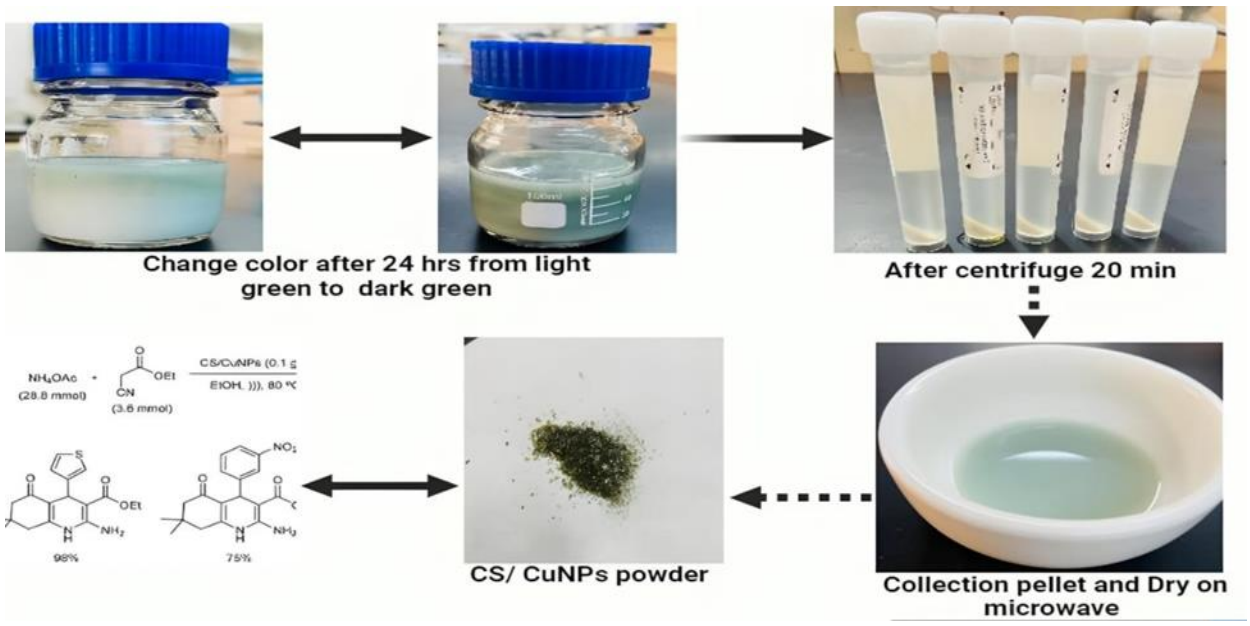

Fig 3. Synthesis of Chi-CuNPs nanoparticles using a biological method.

Characterization of Chi-CuNPs

Physical Characteristics

In this study, metal-vapor synthesis was employed for the preparation of copper nanoparticles, which were subsequently used to fabricate chitosan–copper nanocomposites (Chi-CuNPs). X-ray fluorescence (XRF) analysis confirmed the presence and concentration of copper (%wt) in the synthesized Cu-Chitosan composite. To further analyze particle size and particle distribution, additional characterization techniques were applied.

UV-Visible (UV-Vis) Spectroscopy

UV-Vis spectroscopy is a valuable tool for confirming the formation and stability of metal nanoparticles in aqueous solutions. The UV-Vis spectra of the synthesized nanoparticles, as shown in figure 4a, demonstrated that chitosan effectively facilitated the production of bimetallic nanoparticles. The nanoparticles exhibited a characteristic absorption peak at 207 nm (Fig. 4b), indicating the successful synthesis and stability of the Chi-CuNPs.

Zeta Potential Analysis

The synthesized samples were subjected to zeta potential and particle size measurements using a Malvern Zetasizer 3000 (UK, Malvern Instruments). For this analysis, 100 µL of the nanoparticle suspension was re-dispersed in 900 mL of Milli-Q water and placed into the measurement cuvette. The experiment was conducted at 25°C with a scattering angle of 90°. The refractive index and material dispersion were set at 1.330 and 1.365, respectively, with a viscosity of 0.8872 cP and a dielectric constant of 78.5.

Zeta potential measurements were performed to assess the surface charge and stability of the nanoparticles. As shown in figure 5a, the synthesized CS-CuNPs exhibited a negative zeta potential of -35.36 ± 0.6 mV. This negative surface charge is attributed to the presence of carboxylic and amino functional groups on the surface of the copper nanoparticles. Zeta potential is a critical indicator of colloidal stability; generally, nanoparticles with zeta potential values greater than ±30 mV are considered to form stable dispersions (Reference 24). High zeta potential values demonstrate improved stability of the CuNPs in aqueous solutions, especially when stabilized with chitosan.

In addition, the particle size distribution (hydrodynamic diameter) of the synthesized Chi-CuNPs was assessed using dynamic light scattering (DLS) with the Malvern Zetasizer Nano Series. The average particle size was measured to be approximately 495.17 nm, based on the mean value from three independent runs, all conducted at 25°C (Fig. 5b).

The zeta potential of the colloidal solution, which depends on surface charge, electric potential, and electrostatic repulsion among nanoparticles, was found to be +23.6 mV in certain conditions, suggesting moderate stability and confirming the potential suitability of the product for biomedical applications.

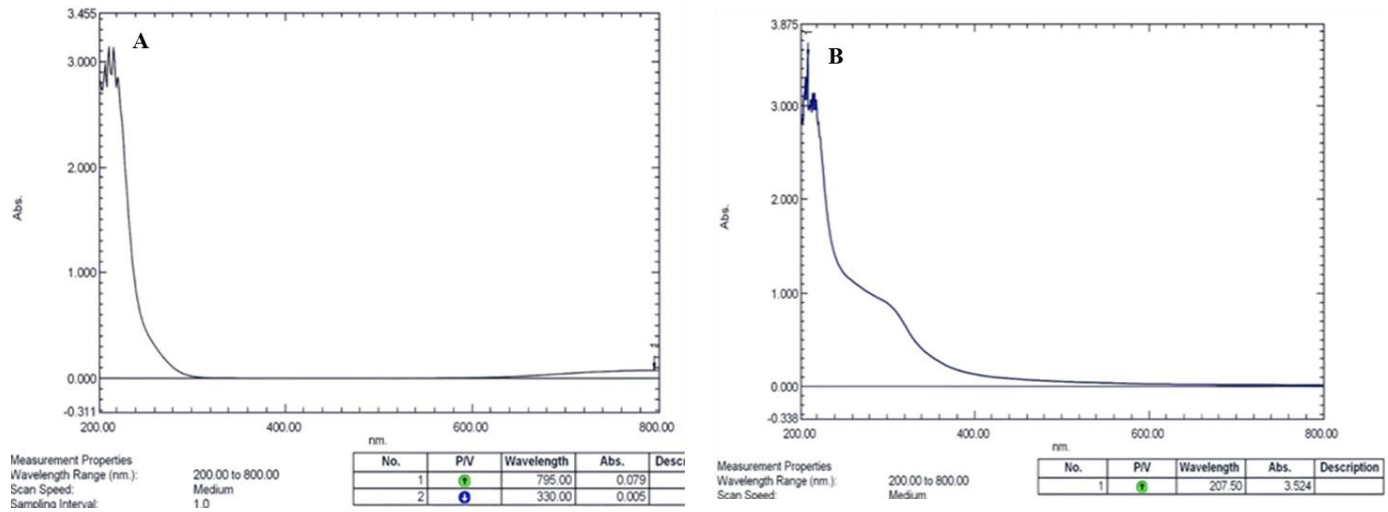

Fig 4. UV–vis spectroscopy analysis of Chi-CuNPs nanoparticles. (A) UV–vis spectra showing the formation of Chi-CuNPs. (B) Band maxima observed at 207 nm confirming nanoparticle synthesis and stability.

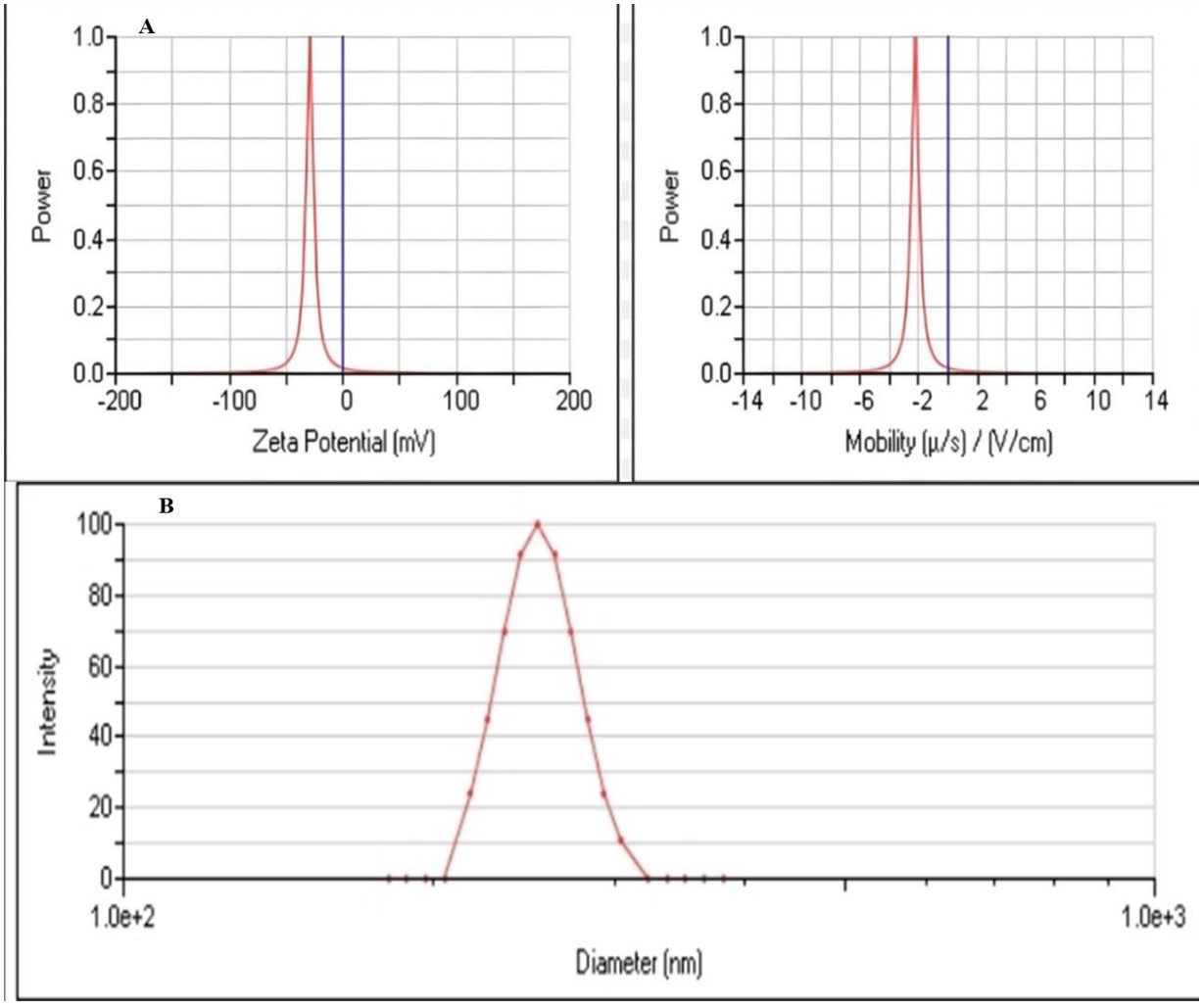

Fig 5. Zeta potential and particle size distribution analysis of Chi-CuNPs. (a) Zeta potential measurement showing a negative surface charge of -35.36 ± 0.6 mV, indicating good colloidal stability. (b) Dynamic light scattering (DLS) results showing an average particle size of approximately 495.17 nm.

Atomic Force Microscopy (AFM) Analysis

AFM analysis of CS-CuNPs was conducted using a CSPM system to identify and characterize the nanoparticle distribution. The microstructure of the chitosan-copper nanocomposite was examined using atomic force microscopy (AFM), revealing that the CS-CuNPs exhibited irregular, triangular cluster morphologies. Based on three-dimensional AFM imaging, the nanoparticles showed an average diameter of approximately 62.54 nm, as confirmed by particle size analysis (Fig. 6).

AFM allows for both three-dimensional surface profiling with atomic-level resolution and quantification of the nano-Newton scale forces exerted by the sample surface on the AFM tip. According to the AFM measurements, the presence of copper oxide (CuO) in the system influenced the surface roughness and topography of the samples. The roughness values for both types of samples were comparable, although variations in their surface textures were observed. Notably, the AFM results qualitatively correlate with the scanning electron microscopy (SEM) findings, confirming the surface morphology.

Additionally, contact angle measurements were carried out to evaluate the wettability of the solid surfaces of both hybrid copper coatings. The contact angles for water droplets on the copper and chitosan-coated samples were measured at 116° and 121°, respectively. These results indicate that both coatings exhibit low surface wettability. However, compared to the pure copper layer, which had a contact angle of 94°, the hybrid samples demonstrated increased hydrophobicity, suggesting that the combination of copper and chitosan enhances the surface's water-repellent properties.

X-ray Diffraction (XRD) Analysis

The XRD patterns revealed that pure chitosan exhibits a crystalline structure, while the CS-CuNPs nanocomposites displayed significantly reduced peak intensities, indicating a decrease in crystallinity. The CS-CuNPs showed a hexagonal quartzite-like structure. The similarity between the sample diffraction pattern and the standard reference confirms that the CS-CuNPs possess a hexagonal wurtzite structure, with nine major peaks observed at diffraction angles corresponding to the (100), (002), (101), (102), (110), (103), (200), (112), and (201) planes.

The aim of this part of the research was to investigate the effect of chitosan modification on copper nanoparticles by synthesizing Cu/chitosan nanocomposites using different molar ratios of copper and chitosan (Fig. 7 a and b).

Furthermore, XRD analysis showed that when chitosan forms nanoparticles (CNPs) through ionic cross-linking with TPP (tripolyphosphate), its characteristic broad peaks at approximately $2\theta \approx 11°$ and 19.6° are largely diminished or disappear entirely. This observation confirms successful nanoparticle formation and structural modification of chitosan. (Table 1).

Energy Dispersive X-ray (EDX) Analysis

Energy Dispersive X-ray (EDX) analysis confirmed the presence of CS-Cu NPs within the polymer matrix of the CS-Cu NPs nanocomposite film (Fig. 8). EDX profiling was performed on a specific region of the coating containing cylindrical particles. The distinct copper (Cu) peaks observed in the spectra confirmed the successful incorporation of CS-Cu NPs into the polymer matrix.

Additionally, the presence of CuO was detected during the elemental analysis of the nanocomposite, further verifying the formation of copper-based nanoparticles within the system.

It has been reported that metallic nanoparticles possess a wide range of applications in agriculture, with the potential to replace hazardous chemical pesticides and fungicides by enhancing the activity of naturally derived compounds. The use of nanotechnology in agricultural formulations offers several advantages, including increased surface area, higher size-to-volume ratio, improved efficacy, and enhanced precision.

In this study, copper nanobiocomposites were successfully synthesized using ascorbic acid, a natural organic compound, along with chitosan, a naturally occurring biopolymer. (see table 2)

Field Emission Scanning Electron Microscope (FESEM) and Transmission Electron Microscopy (TEM) Analysis

FESEM and TEM analyses were used to reveal the morphological distribution, including size and shape, as well as the elemental structure of the synthesized samples. The scanning electron microscope measured the size and shape of the nanoparticles. SEM images were captured at magnifications of 5,000x and 10,000x.

Figure 9a shows images of the Chi-Cu nanoparticles. The figure illustrates that most Chi-Cu NPs exhibit smooth surfaces and flake-like shapes, with particle sizes reaching up to 50 nm. Similarly, SEM images of Chi-Cu metal nanoparticles taken at 5,000x magnification (Fig. 9b) show that most Chi-Cu metal NPs also possess flake-like morphologies, consistent with the observations for Chi-Cu NPs.

Fourier Transform Infrared Spectra Measurement (FTIR)

Fourier Transform Infrared Spectroscopy (FTIR) was used to analyze the biosynthesized Chi-CuNPs. The FTIR spectrum showed a peak at 1156 cm^{-1}, which was assigned to the saccharide structure. A strong signal at 1350 cm^{-1} was attributed to the -CH_3 group in the amide. The large peaks at 1021 cm^{-1} and 1098 cm^{-1} indicated the C–O stretching vibration of chitosan, while the peaks at 1675 cm^{-1} and 1600 cm^{-1} corresponded to the -C=O and -NH_2 stretching vibrations of amide I and II, respectively. The absorption band at 1200 cm^{-1} was identified as the antisymmetric stretching of the C–O–C bridge, and the bands between 1100 cm^{-1} and 1020 cm^{-1} were related to skeletal vibrations associated with C–O stretching.

Overall, the results indicate that the FTIR spectra of synthetic and extra-pure chitosan are nearly identical. This confirms that chitosan was effectively extracted from the leftover shrimp shells, as shown in Figure 10 (a, -c), representing copper sulfate, chitosan, and Chi-CuNPs, respectively (table 3).

Antibacterial and Antifungal Activity of Chi-CuNPs

Chitosan-stabilized metallic nanoparticles have attracted significant research interest due to the inherent antimicrobial properties of chitosan, both alone and when combined with metal nanoparticles. Chitosan exhibits excellent antibacterial properties, and several mechanisms have been proposed by researchers to explain its antimicrobial activity.

The antibacterial activity of the synthesized chitosan-copper nanoparticles (Chi-CuNPs) was tested against four Gram-negative bacterial strains, as depicted in figure 11 (A-E) and figure 12 (A-C supplementary), representing Gram-negative bacteria, Gram-positive bacteria, and *Candida* species, respectively.

The standard drug Kanamycin (1000 µg/mL) exhibited inhibition zones of 24 mm, 25 mm, 26 mm, 27 mm, 27 mm, and 24 mm against *Pseudomonas aeruginosa, Klebsiella pneumoniae, Salmonella typhi, Shigella* spp., *Proteus mirabilis*, and *Escherichia coli*, respectively. Additionally, against *Enterococcus faecium*, the inhibition zone at the same concentration ranged between 29–30 mm.

Table 1- X-ray Diffraction (XRD) analysis of chitosan showing characteristic diffraction peaks indicating the crystalline structure of chitosan.

Pos. [°2Th.]	Height [cts]	FWHM Left [°2Th.]	d-spacing [Å]	Rel. Int. [%]	Tip Width	Matched by
10.2(1)	769(17)	5.0(2)	8.62906	58.24	6.0039	
10.3(1)	385(17)	5.0(2)	8.62906	29.12	6.0039	
20.94(1)	1321(11)	5.26(5)	4.23969	100.00	6.3087	
20.99(1)	660(11)	5.26(5)	4.23968	50.00	6.3087	

Table 2: Energy Dispersive X-ray (EDX) analysis showing the elemental composition of CS-CuNPs nanocomposites, confirming the successful incorporation of copper nanoparticles within the chitosan matrix.

Element	Line Type	Apparent Concentration	k Ratio	Wt%	Wt% Sigma	Atomic %	Standard Label	Factory Standard
C	K series	3.29	0.03285	45.39	0.36	54.31	C Vit	Yes
O	K series	8.85	0.02977	48.74	0.35	43.78	SiO2	Yes
Cl	K series	0.70	0.00608	3.26	0.08	1.32	NaCl	Yes
Cu	L series	0.25	0.00251	2.62	0.17	0.59	Cu	Yes
Total:				100.00		100.00		

For antifungal activity, Chi-CuNPs were tested against *Candida glabrata*, *Candida krusei*, and *Candida albicans*, with inhibition zones ranging from 21–24 mm at a concentration of 1000 µg/mL. Among the tested *Candida* species, *Candida krusei* showed the highest sensitivity to Chi-CuNPs, exhibiting the largest zone of inhibition compared to Candida glabrata and Candida albicans.

Moreover, a statistically significant difference ($p < 0.05$) in the mean inhibition zones was observed among *Candida albicans, Candida krusei, and Candida glabrata* following treatment with Chi-CuNPs at concentrations between 500 and 1000 µg/mL. No zone of inhibition was detected at lower concentrations.

The cytotoxic effect of CS-Cu NPs nanoparticles on tumor cell lines

The cytotoxic activity of chitosan-copper oxide nanoparticles on the human breast adenocarcinoma cell line MCF7 were studied as seen in figure 13. Morphology of control cell and treatment cell with two concentration (50 ug/ml and 100 ug/ml) . The results obtained showed that the cell viability reduced as the concentration of CS-CuNPs increased. The GI 50 value of CS-CuNPs was about 24. 5 µg/ml. These NPs exhibited toxic effects against the MCF7 cell line, and at a concentration of 25 µg/ml, the cytotoxic effects reached 65.4%. CS-CuNPs were tested for *in vitro* cytotoxicity against MCF7 cell lines at concentrations of 6.25–100 µg/ml; In agreement with our results, several evidence have indicated the cytotoxic potential of CS-CuNPs on different cell lines (Table 4) The interactions being expressed as cell viability (%) was observed at different CS-Cu NPs concentrations (6.25–100 µg/mL) with the four cell lines which have been shown in figure 14.In all the cases the % cell viability gets reduced with increasing nanocomposite concentrations.

Discussion

One of the most pressing concerns in modern healthcare is the rise of antibiotic resistance, which makes it increasingly difficult for existing antibiotics to combat drug-resistant organisms. Furthermore, biofilm formation provides an additional protective barrier for these pathogens, posing significant challenges to the healthcare sector due to persistent infections caused by drug-resistant, biofilm-forming microorganisms (Ahmed et al. 2024).

Table 3 FTIR spectral data showing the characteristic functional groups of copper sulfate, chitosan, and biosynthesized Chi-CuNPs.

	Peak	Intensity	Corr. Intensity	Base (H)	Base (L)	Area	Corr. Area
1	403.12	58.528	0.326	480.28	399.26	17.526	0.335
2	596	60.933	5.648	796.6	489.92	57.403	5.062
3	896.9	69.238	0.396	902.69	858.32	6.755	0.07
4	1022.27	63.128	4.932	1138	902.69	43.825	4.516
5	1157.29	66.751	1.54	1284.59	1138	22.063	1.14
6	1313.52	75.156	0.152	1315.45	1284.59	3.624	0
7	1365.6	73.888	1.986	1396.46	1340.53	6.995	0.296
8	1423.47	74.687	0.802	1440.83	1411.89	3.593	0.067
9	1514.12	71.053	1.045	1519.91	1477.47	5.522	0.079
10	1635.64	68.291	12.299	1824.66	1560.41	26.718	7.614
11	2067.69	96.893	0.021	2260.57	2065.76	1.715	-0.097
12	2308.79	97.63	1.581	2355.08	2260.57	0.592	0.264
13	2856.58	88.241	1.309	2899.01	2355.08	21.499	6.787
14	3404.36	92.849	0.339	3547.09	3396.64	3.365	0.614

The hemostatic capabilities of chitosan nanoparticles (CS-NPs) are attributed to their net positive charge, which depends on the degree of protonated amine groups and the deacetylation degree (DD) (Huet al. 2018). To synthesize metal nanoparticles based on chitosan, a modified solution casting method was employed, producing two distinct types of nanoparticles, Chi-Zn and Chi-Cu, each differing in size and morphology based on the raw materials used (Hu et al. 2018).

A novel PPCSB system has been developed to serve as both a functional stabilizer and delivery platform, enhancing the targeted antibacterial efficacy of CuNPs. The current study addresses key challenges in antibacterial therapy by synergistically combining these components, providing a foundation for safe, effective, and environmentally sustainable treatments to combat bacterial resistance (Islam et al. 2024).

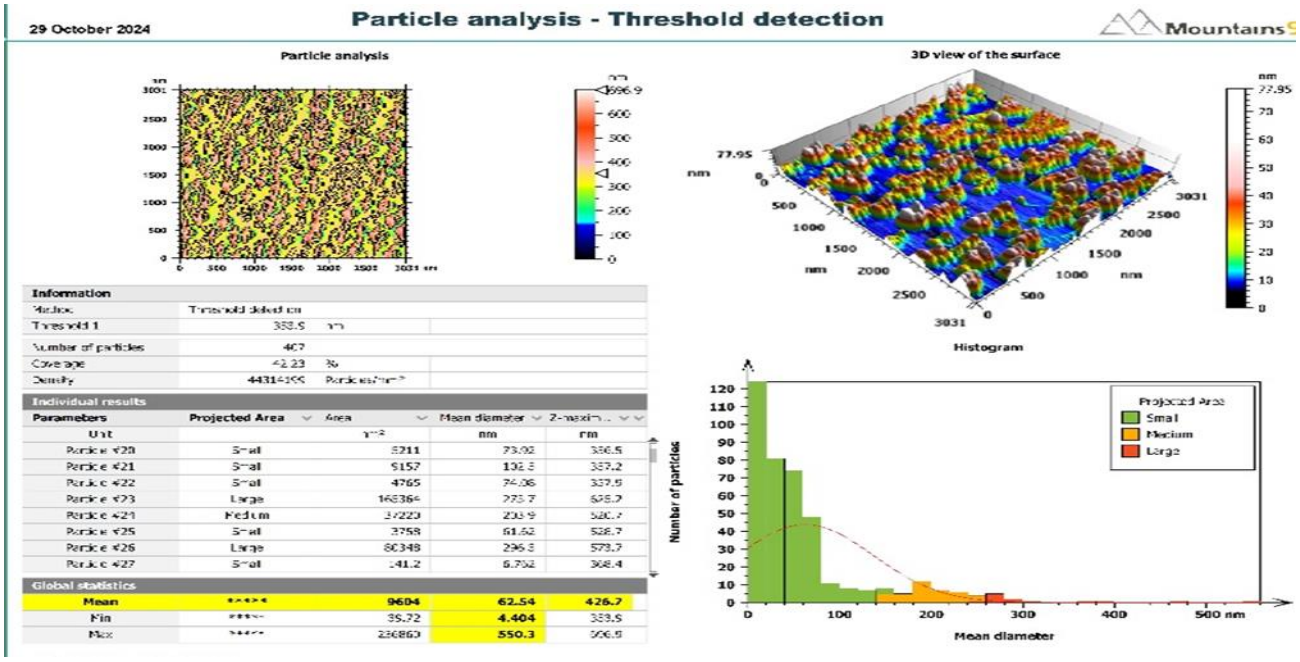

Fig 6. Atomic Force Microscopy (AFM) analysis showing the surface morphology and size distribution of CS-Cu nanoparticles (CS-Cu NPs).

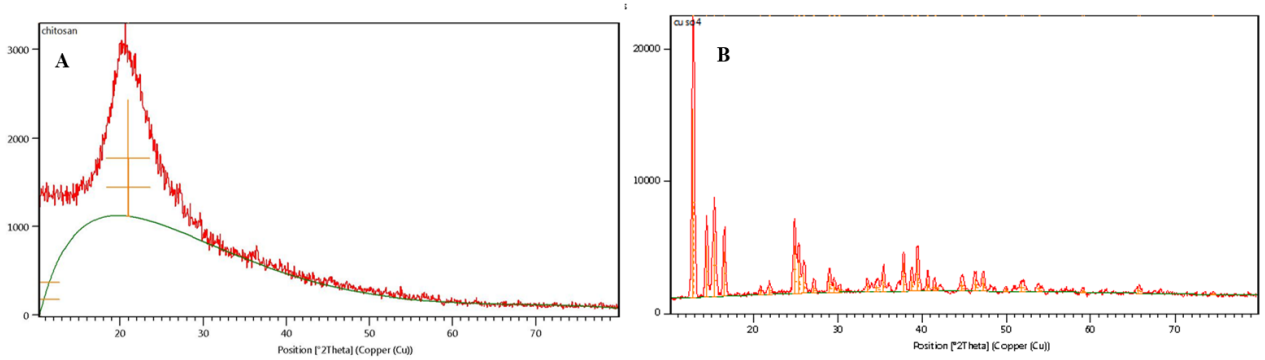

Fig 7. X-ray Diffraction (XRD) analysis of (a) pure Chitosan and (b) CS-Cu NPs, illustrating the crystallinity and structural characteristics of the synthesized nanoparticles.

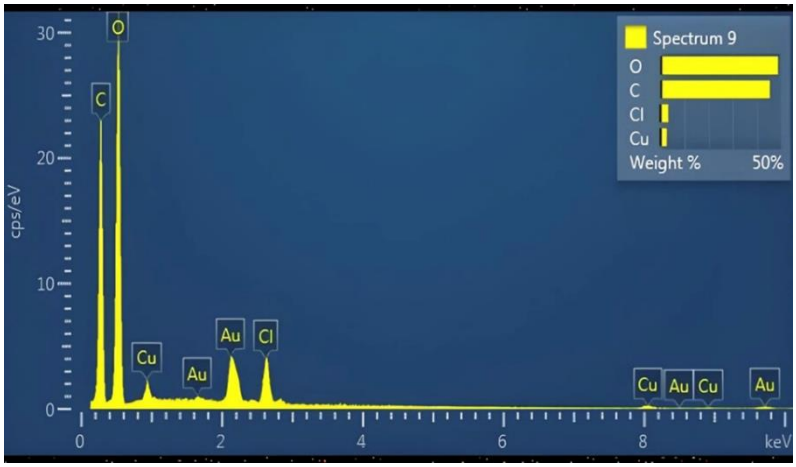

Fig 8. Energy Dispersive X-ray (EDX) analysis of CS-Cu NPs confirming the elemental composition and successful incorporation of copper nanoparticles into the chitosan matrix.

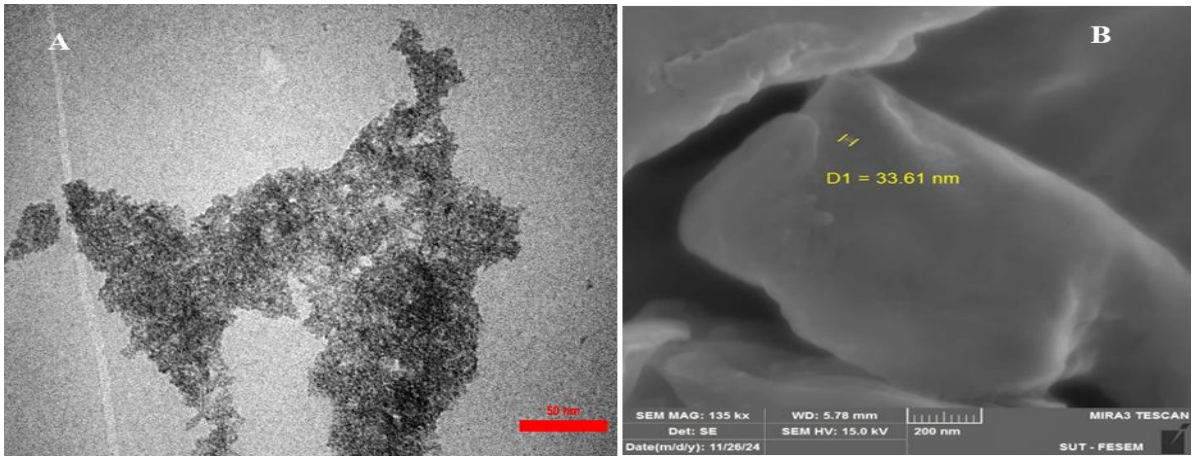

Fig 9. Morphological characterization of Chitosan-Cu NPs by (a) Field Emission Scanning Electron Microscopy (FESEM) and (b) Transmission Electron Microscopy (TEM).

Copper nanoparticles play a crucial role in suppressing the inflammatory responses associated with chitosan and in supporting collagen synthesis via copper-dependent enzymes, both of which are essential for promoting wound healing (Alqahtani et al. 2024). Incorporating nano-copper (nCu) with chitosan enhances its wound-healing potential, as chitosan's polycationic nature in acidic conditions enables effective bonding with metallic ions like Cu (Mohamed et al. 2024).

The present study explored the antibacterial and anticancer properties of CH, CuO, and CH-CuO nanoparticles. Various techniques were used to characterize these green-synthesized nanoparticles. SEM and TEM analyses revealed predominantly spherical nanoparticles with average sizes of 62 nm (CH), 35 nm (CuO), and 51 nm (CH-CuO), consistent with previous findings (Maheo et al. 2022).

When comparing the antioxidant activity of chemically synthesized and green-synthesized CuO nanoparticles, the biologically synthesized nanoparticles exhibited superior activity. Chitosan's structure contains amino groups capable of donating hydrogen ions, effectively scavenging free radicals. Consequently, the antioxidant activity of CH-CuO nanoparticles was significantly enhanced due to the combined effects of chitosan and green synthesis (Ivanova et al. 2022).

To evaluate antibacterial efficacy, chitosan-stabilized copper nanoparticles were synthesized and tested against both Gram-positive and Gram-negative bacteria. The results demonstrated that chitosan-stabilized CuNPs exhibited greater activity against Gram-negative bacteria, likely due to differences in cell wall composition (Verma et al. 2021), consistent with the findings of (Hongfeng et al. 2021).

The biological potential of CS-CuNPs, including their anticancer properties, was also investigated. Significant cytotoxic effects were observed against major human bladder cancer cell lines, such as TCCSUP (Grade IV, transitional cell carcinoma), SCaBER (squamous cell carcinoma), and UM-UC-3 (transitional cell carcinoma). In lung cancer studies, the nanocomposite was tested on well-differentiated bronchogenic adenocarcinoma (HLC-1), moderately differentiated adenocarcinoma (LC-2/ad), and poorly differentiated adenocarcinoma (PC-14) cell lines using the MTT assay. A dose-dependent reduction in cancer cell viability was observed in the presence of the Fe_3O_4/CS/Cu(II) nanocomposite (Shi et al. 2021).

Chitosan's excellent chelating properties stem from its functional -NH_2 and -OH groups. Various factors influence the size and morphology of metallic nanoparticles, including chitosan content, molecular weight, reaction time, degree of acetylation, pH of the medium, synthesis process, and the type of chitosan derivative used. The size and shape of nanoparticles significantly affect their properties and applications.

This study also focused on the green synthesis of CS/PVA-coated CuO nanoparticles (CS/PVA/CuONCs) using Anacardium occidentale (cashew) fruit extracts. The synthesized nanocomposites were characterized using FTIR, XRD, FESEM-EDX, and UV-Vis spectroscopy. The antibacterial and antioxidant activity of CS/PVA/CuONCs was assessed against both Gram-positive and Gram-negative bacteria. Additionally, anti-inflammatory, anti-diabetic, and anti-cholinergic properties were evaluated, along with the anticancer and hemolytic activity of the nanocomposites. This research presents an eco-friendly approach for developing nanocomposites with promising therapeutic potential, employing green synthesis techniques and biocompatible polymers (Rajkumar et al. 2025).

A

	Peak	Intensity	Corr. Intensity	Base (H)	Base (L)	Area	Corr. Area
1	403.12	58.528	0.326	480.28	399.26	17.526	0.335
2	596	60.933	5.648	796.6	489.92	57.403	5.062
3	896.9	69.238	0.396	902.69	858.32	6.755	0.07
4	1022.27	63.128	4.932	1138	902.69	43.825	4.516
5	1157.29	66.751	1.54	1284.59	1138	22.063	1.14
6	1313.52	75.156	0.152	1315.45	1284.59	3.624	0
7	1365.6	73.888	1.986	1396.46	1340.53	6.995	0.296
8	1423.47	74.687	0.802	1440.83	1411.89	3.593	0.067
9	1514.12	71.053	1.045	1519.91	1477.47	5.522	0.079
10	1635.64	68.291	12.299	1824.66	1560.41	26.718	7.614
11	2067.69	96.893	0.021	2260.57	2065.76	1.715	-0.097
12	2308.79	97.63	1.581	2355.08	2260.57	0.592	0.264
13	2856.58	88.241	1.309	2899.01	2355.08	21.499	6.787
14	3404.36	92.849	0.339	3547.09	3396.64	3.365	0.614

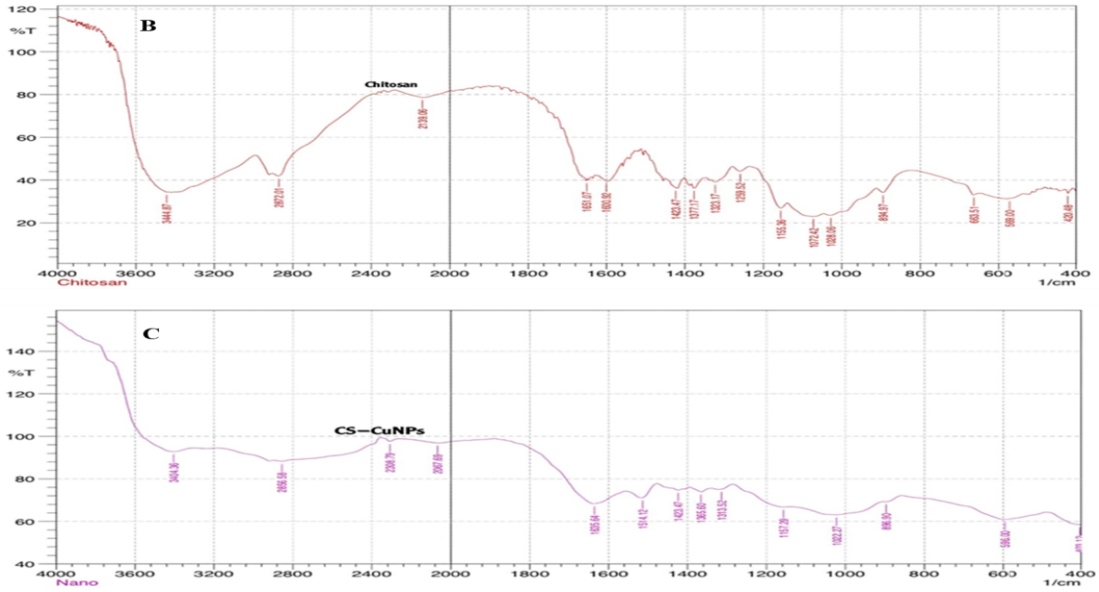

Fig 10. Fourier Transform Infrared (FTIR) Spectra of (a) Copper sulfate, (b) Chitosan, and (c) Chi-CuNPs.

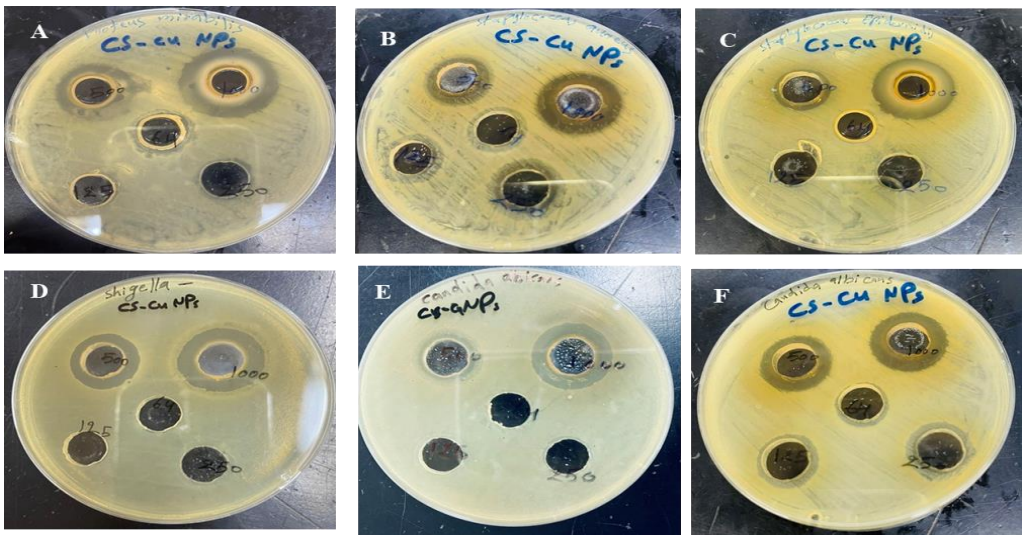

Fig 11. Zones of microbial inhibition against MIC Chi-CuNPs at concentrations of 1000, 500, 250, 125, and 64 µg/mL: (a) P. mirabilis, (b) S. aureus, (c) S. epidermidis, (d) Shigella spp., (e) Candida krusei, and (f) C. albicans.

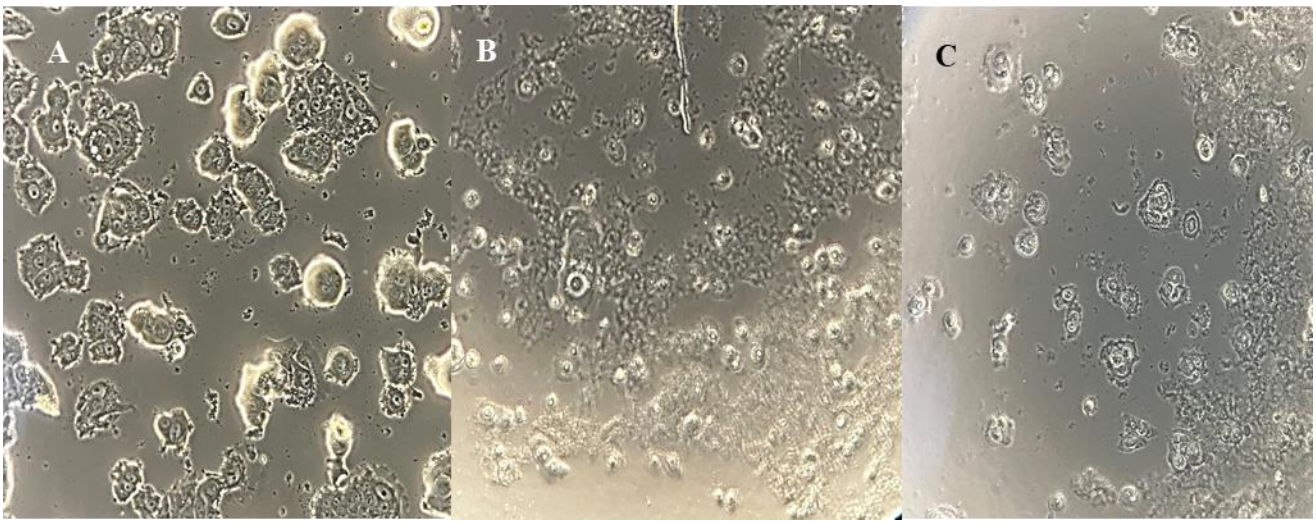

Fig 13. The cytotoxic effect of CS-CuNPs on MCF-7 cells: (a) Control (untreated) cells, (b) cells treated with 50 µg/mL, and (c) cells treated with 100 µg/mL.

Table 4 Effect of different concentrations of CS-CuNPs (6.25–100 µg/mL) on the viability of MCF-7 cell lines, expressed as percentage cell viability.

		CV	6.25µg/ml	12.5µg/ml	25µg/ml	50 µg/ml	100µg/ml
CHCU TR1	Raw data	0.305	0.136	0.106	0.201	0.154	0.148
	% survival	100	44.590	34.754	65.901	50.491	48.524
		CV	**6.25µg/ml**	**12.5µg/ml**	**25µg/ml**	**50 µg/ml**	**100µg/ml**
CHCU TR2	Raw data	0.305	0.346	0.299	0.128	0.146	0.132
	% survival	100	113.442	98.032	41.9672	47.8688	43.278
		CV	**6.25µg/ml**	**12.5µg/ml**	**25µg/ml**	**50 µg/ml**	**100µg/ml**
CHCU TR3	Raw data	0.305	0.275	0.265	0.132	0.163	0.158
	% survival	100	90.163	86.885	43.278	53.442	51.803

Where: CV: Control vehicle, TR: technical replicate.

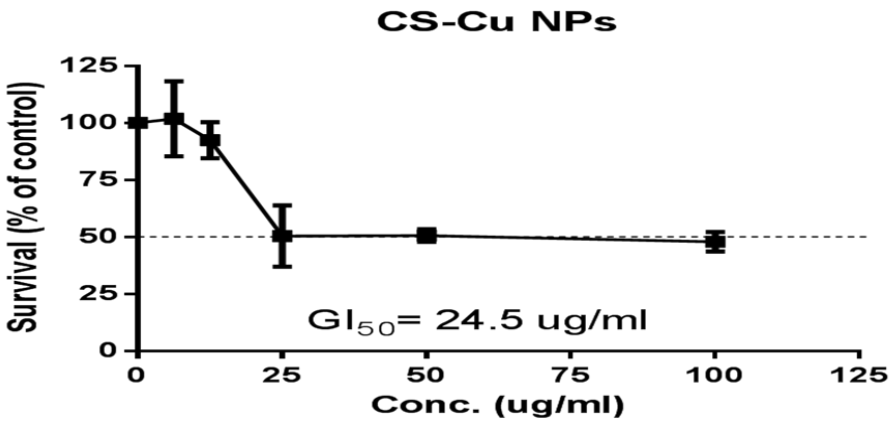

Fig 14. The cytotoxic effect of CS-CuNPs on MCF-7 cells.

Conclusion

Chitosan, a natural biopolymer, has proven to be an effective host material for synthesizing metallic nanoparticles (MNPs) due to its excellent stabilizing and capping abilities, biocompatibility, biodegradability, eco-friendliness, and non-toxic nature. The green, time-efficient, and cost-effective method presented in this study offers significant advantages for the synthesis of chitosan nanoparticles, which hold potential for applications as antimicrobial and therapeutic agents.

This study compared the antibacterial, antibiofilm, and anticancer properties of CH, CuO, and CH-CuO nanoparticles produced via green synthesis. The nanoparticles demonstrated significant efficacy against multidrug-resistant bacteria and biofilm-forming pathogens. These findings contribute to the development of chitosan-stabilized metallic nanoparticles and their optimization for various biomedical applications, particularly in combating highly resistant microbes and harmful parasites. The study also highlights the unique properties, advantages, limitations, and factors influence.

Conflict of interest

No conflicts of interest, as the authors declared.

Funding source:

No governmental, commercial, or nonprofit funding agencies provided any funds for this project.

References:

Abdel-Azeem A, Nada A, O'Donovan A, Thakur V K, Elkelish A. (2020a). Mycogenic Silver Nanoparticles from Endophytic *Trichoderma atroviride* with Antimicrobial Activity. Journal of Renewable Materials, 8(2): 171-185

Ahmed M E, Al-Awadi A Q. (2024). *Enterococcus faecium* Bacteriocin efflux pump mexa gene and promote skin wound healing in mice. *Journal of microbiology, biotechnology and food sciences*, e10711-e10711.

Ahmed ME, Al-Awadi AQ, Abbas AF. (2023).Focus of Synergistic Bacteriocin-Nanoparticles Enhancing Antimicrobial Activity Assay. *Microbiological journal. (6)*. P. 95—104. https://doi.org/10.15407/microbiolj85.06.095.

Alhammer AH, Al-junior SI, Mudhafar SA.(2024). APR-246 enhances the anticancer effect of doxorubicin against p53-mutant AsPC-1 pancreatic cancer cells. *Baghdad Sci* J 21: 2551-2560.

Alqahtani N F. (2024). Synthesis and characterization of a new nano-antibiotic integrating polyphosphonium chitosan Schiff base and copper nanoparticles for bacterial infection therapy. *Materials Today Communications*, 111385.

Ameh T, Gibb M, Stevens D, Pradhan SH, Braswell E, Sayes CM. (2022).Silver and copper nanoparticles induce oxidative stress in bacteria and mammalian cells. *Nanomaterials*.12(14):2402.

Ardila N, Daigle F, Heuzey M, Abdellah A.(2017).Antibacterial Activity of Neat Chitosan Powder. *Molecules* , 22, 100.

Ashokkumar M, Palanisamy K, Ganesh Kumar A, Muthusamy C, Senthil Kumar K J. (2024). Green synthesis of silver and copper nanoparticles and their composites using *Ocimum sanctum* leaf extract displayed enhanced antibacterial, antioxidant and anticancer potentials. *Artificial Cells, Nanomedicine, and Biotechnology*, 52(1), 438-448.

Diksha D, Gupta SK, Gupta P, Banerjee UC, Kalita D, Gupta S.(2023). Antibacterial Potential of Gold Nanoparticles Synthesized From Leaf Extract of *Syzygium cumini* Against Multidrug-Resistant Urinary Tract Pathogens. *Cureus*. 2023;15(2).

Faiq NH, Ahmed M E. (2024). Inhibitory Effects of Biosynthesized Copper Nanoparticles on Biofilm Formation of *Proteus mirabilis*. *Iraqi Journal of Science*, 65-78

Fawzi F H, Ahmed M E. (2024). Green Synthesis and Characterization of Selenium Nanoparticles via *Staphylococcus warneri* Approach: Antimicrobial and on PhzM Pyocyanin Gene Expression in Pseudomonas aeruginosa. *Plasmonics*, 1-17. https://doi.org/10.1007/s11468-024-02378-2

Gezaf S., Hamedo H., Ibrahim A, Mossa M. (2022). Mycosynthesis of silver nanoparticles by endophytic Fungi: Mechanism, characterization techniques and their applications. *Microbial Biosystems*, 7(2), 48-65. doi: 10.21608/mb.2023.185718.1066

Hassan Z J S, Hamid M K, Ahmed M E. (2022). Synthesized Zinc Oxide Nanoparticles by the Precipitation Method on *Streptococcus* spp. from Dental Carries and Cytotoxicity Assay. Int. J. Drug Deliv. *Technol*, 12, 1327-1330

Hongfeng Z, El-Kott A, Ahmed A E, Khames A. (2021). Synthesis of chitosan-stabilized copper nanoparticles (CS-Cu NPs): Its catalytic activity for CN and CO cross-coupling reactions and treatment of bladder cancer. *Arabian Journal of Chemistry*, 14(10), 103259.

Hu Z, Lu S, Cheng Y, Kong S, Li S, Li C, Yang L.(2018). Investigation of the Effects of Molecular Parameters on the Hemostatic Properties of Chitosan. *Molecules* , 23, 3147.

Islam G J, Zannah S, Mohinuddin M. (2024). Chitosan Based Copper (II) and Cadmium Nanoparticles: Synthesis, Characterization, and Investigation of Antibacterial Activity. *International Journal of Research and Scientific Innovation*, 11(6), 543-561.

Ivanova D G, Yaneva Z L. (2020). Antioxidant properties and redox-modulating activity of chitosan and its derivatives: biomaterials with application in cancer therapy. *BioResearch Open Access* 9, 64–72. doi: 10.1089/biores.2019.0028.

Kadhim ZH, Ahmed ME, Şimşek I. (2023). "Biologically synthesized copper nanoparticles from S. epidermidis on resistant S. aureus and cytotoxic assay," Bionatura, vol. 8, no. 1. https://doi.org/10.21931/RB/CSS/2023.08.01.54

Kadhim ZH, Ahmed ME. (2023). Antibacterial and Cytotoxic Effect of Synthesized CuoNPs from *Staphylococcus epidermidis*. *Iraqi Journal of Biotechnology*,. 22, (1), 173-182.

Mahdi SM, Abbas AF, Ahmed ME. (2024). Cytotoxicity of zinc oxide nanoparticles to lymphocytes using Enterococcus faecium bacteriocin and assessment of their antibacterial effects. *Nanomed Res* J; 9(2): 180-194. DOI: 10.22034/nmrj.2024.02.007

Maheo A R, Vithiya B S M, Prasad T A A, Tamizhdurai, P, Mangesh V. (2022). Biosynthesis, characterization, biological and photo catalytic investigations of *Elsholtzia blanda* and chitosan mediated copper oxide nanoparticles. *Arab. J. Chem.* 15:103661. doi: 10.1016/j.arabjc.2021.103661.

Mallick S, Sharma S, Banerjee M, Ghosh S S, Chattopadhyay A, Paul A. (2012). Iodine-stabilized Cu nanoparticle chitosan composite for antibacterial applications. *ACS applied materials & interfaces*, 4(3), 1313-1323.

Mohamed HI, Mahmoud NMR, Ramadan A, Al-Subaie AM, Ahmed SB.(2024). Novel Biological-Based Strategy for Synthesis of Green Nanochitosan and Copper-Chitosan Nanocomposites: Promising Antibacterial and Hematological Agents. *Nanomaterials.* 14(13):1111. https://doi.org/10.3390/nano14131111

Mossa M, Gezaf S, Ibrahim A, Hamedo H. (2024). Preliminary screening of endophytic fungi hosted some wild plants in North Sinai for biogenic production of silver nanoparticles. *Microbial Biosystems*, 8(2), 57-73. doi: 10.21608/mb.2024.341385

Muzammil S, Hayat S, Fakhar-E-Alam M, Aslam B, Siddique MH, Nisar MA et al.(2018). Nanoantibiotics: Future nanotechnologies to combat antibiotic resistance. *Front Biosci*. ;10:352-74.

Rajkumar M, Presley SD, Govindaraj P, Kirubakaran D, Farahim F, Ali T, Shkir M, Latha S. (2025). Synthesis of chitosan/PVA/copper oxide nanocomposite using *Anacardium occidentale* extract and evaluating its antioxidant, antibacterial, anti-inflammatory and cytotoxic activities. *Scientific Reports,* 15(1), 3931.

Romi ZM, Ahmed ME. (2024). The Influence of Biologically Synthesized Copper Nanoparticles on the Biofilm Produced by *Staphylococcus haemolyticus* 1solated from Seminal Fluid. *Iraqi Journal of Science,* 1948-1968.

Salman MF, ME AM. (2024). The effect of selenium nanoparticles on the expression of MexB gene of Pseudomonas aeruginosa Isolated from wound and burn infections. *Iraqi JMS.* 22 (1): 79-92. doi: 10.22578. IJMS, 22(10).

Shi Z, Mahdavian Y, Mahdavian Y, Mahdigholizad S, Irani P, Karimian M, Abbasi N, Ghaneialvar H, Zangeneh A, Zangeneh MM. (2021). Cu immobilized on chitosan-modified iron oxide magnetic nanoparticles: Preparation, characterization and investigation of its anti-lung cancer effects. *Arabian Journal of Chemistry*, 14(8), 103224.

Srivastava S, Usmani Z, Atanasov AG, Singh VK, Singh NP, Abdel-Azeem AM, Prasad R, Gupta G, Sharma M, Bhargava A. (2021). Biological Nanofactories: Using Living Forms for Metal Nanoparticle Synthesis. *Mini-Reviews in Medicinal Chemistry*, 21, 245-265

Tabesh ES, Salimijazi HR, Kharaziha M, Mahmoudi M, Hejazi M.(2019). Development of an In-Situ Chitosan-Copper Nanoparticle Coating by Electrophoretic Deposition. Surf. Coat. *Technol.* 364, 239–247.

Usman MS, Ibrahim NA, Shameli K, Zainuddin N, Yunus WM. (2012). Copper nanoparticles mediated by chitosan: synthesis and characterization via chemical methods. *Molecules,* 17(12), 14928-14936.

Verma DK, Malik R, Meena J, Rameshwari R. (2021). Synthesis, characterization and applications of chitosan based metallic nanoparticles: A review. *Journal of Applied and Natural Science*, 13(2), 544-551.